

Addendum: Tritium Transport at the Rulison Site, a Nuclear-stimulated Low-permeability Natural Gas Reservoir

prepared by

Clay A. Cooper, Ming Ye, and Jenny B. Chapman
Desert Research Institute
Nevada System of Higher Education

And
Rex Hodges
S.M. Stoller Corporation

submitted to

S.M.Stoller Corporation
Office of Legacy Management
U.S. Department of Energy
Grand Junction, Colorado

January 2009

Executive Summary

Project Rulison, located in western Colorado, was the site of a subsurface nuclear test in 1969. An earlier report (Cooper *et al.*, 2007) presented results of a numerical model that suggests there is less than five percent probability of tritium (the radionuclide of primary concern) reaching a hypothetical gas production well located 258 m from the detonation point. Reviews of the model results indicated concerns with the value of the partitioning coefficient controlling the distribution of tritiated water between liquid and vapor phases, the assignment of effective porosity to hydraulically generated fractures surrounding the hypothetical production well, and the treatment of molecular diffusion in the partially saturated reservoir. These concerns are addressed in this addendum through additional computer simulations testing the impact of these model features on the degree to which tritium is transported away from the detonation point.

Independent evaluation of the partitioning coefficient identified that the value used in Cooper *et al.* (2007) was inappropriate for the subsurface temperatures present in the gas reservoir at Rulison. A more correct value leads to no transport of tritium above background to the production well because tritiated water is strongly favored in the immobile liquid phase. The previous model assumed that the hydraulic fractures around the production well had a porosity of ten percent. Reduction of this porosity to that of the host sandstone increases the velocity of the gas phase and accompanying tritiated water vapor. With respect to tritium diffusion, application of a tortuosity value that is constant and greater than the Millington-Quirk saturation-dependent model used previously results in greater diffusive spreading of the tritium plume. Both the hydrofracture porosity and diffusivity changes favor enhanced tritium transport away from the nuclear chimney, but their combined effects are overwhelmed by the effect of the partitioning coefficient, such that the new simulations predict less tritium transport than presented in Cooper *et al.* (2007). Only when partitioning is assumed to occur under the elevated temperature conditions that may be present in the bottom of the nuclear cavity, is transport observed at concentrations higher than that in Cooper *et al.* (2007). These conditions are not representative of the subsurface in the upper nuclear chimney or the surrounding formation. All of the additional simulations and sensitivity tests were performed with only the top ten of the 500 equally probable realizations considered by Cooper *et al.* (2007). Each of the 500 realizations presents an equally likely distribution of sandstone and shale; their porosity, permeability, and the length of the hydrofractured zone were selected from ranges possible for the formations. Focusing on only the ten realizations with the most transport neglects the importance of the sandstone-shale geometry in limiting transport from the nuclear chimney. Only in those few realizations with well-connected sandstone between the nuclear chimney and the production well is there any opportunity for transport. For those low probability cases, the new simulations show that the tritiated water partitioning coefficient is the next dominant factor to control transport. Although low porosity and liquid water contents of the hydrofracture zone and small tortuosity values have the potential to increase tritium transport away from the chimney, they are much less important than the configuration of the sandstone-shale geometry and partitioning of tritiated water between phases. The 500 realizations of sandstone and shale facies developed by Cooper *et al.* (2007) indicate that the probability of direct sandstone connections between the nuclear chimney and future production wells is low, but cannot be ruled out. The evaluation of the partitioning coefficient indicates that strong partitioning into the immobile liquid phase is a likely process that will limit transport, even in the presence of good sandstone connections.

Introduction and Purpose

In late September 2007, the U.S. Department of Energy (DOE) published a report of a numerical model describing radionuclide transport at the site of the Rulison underground nuclear test (Cooper *et al.*, 2007). That report presented calculations of the nature and extent of subsurface tritium contamination from 1969 (the year of the detonation) through 2007. Also reported was an evaluation of tritium migration to a possible future location for a natural gas production well outside the U.S. Department of Energy (DOE) drilling restriction in lot 11. This is an addendum to the Cooper *et al.* (2007) report. It is not intended to be a stand-alone document; rather, it is built upon data, models, and results presented in Cooper *et al.* (2007).

The model presented in Cooper *et al.* (2007) predicts that tritium from the detonation is presently confined to lot 11. The results for the gas production scenario predict that detectable tritium will not reach the hypothetical producing well in over 95 percent of the 500 analyzed permeability/porosity/facies realizations (shortened to “realizations” throughout the rest of this addendum). (A realization is a single computer-generated facies of sandstone and shale with their permeability and porosity values.) The peak mass fraction of tritiated water vapor (mass of tritiated water per mass of gas for a unit volume of gas, defined as X_g^{THO}) in 99 percent of the realizations was low enough that it is likely to be of no risk to the environment.

The Rulison model and results were reviewed by many individuals, both internal and external to the DOE, with expertise in various aspects of subsurface flow and transport. Some comments highlighted issues that were not fully explained in the original report. Comment responses were prepared for the reviewers to clarify these aspects. Other comments concerned the limitations of simulating flow and transport through complex subsurface systems such as fractured sandstone. Fracture flow was handled in the model by assuming that the sandstone formation could be represented as an equivalent porous medium (EPM), which approximates flow through volumetrically small fracture spaces with relatively large grid blocks and appropriate permeability and porosity scaling. The rigorous alternative to an EPM is the simulation of a network of discrete fractures in the sandstone and an attempt to approximate fracture flow with Darcy’s law. The discrete fracture approach has theoretical, as well as practical problems such as lack of data and an inappropriate model for fluid flow through individual fractures and their networks. Nonetheless, a common concern of many reviewers was whether or not the Rulison EPM model adequately captured the potential for rapid flow through fractured rock. Though the existing analysis of many realizations for a range of possible conditions allowed quantification of the uncertainties inherent in the problem, interest focused on the small subset of realizations in which transport occurred to the production well. In other words, subsequent to the results in Cooper *et al.* (2007), the emphasis turned from assessing probable tritium transport behavior to evaluating low probability, but potentially high consequence, events.

The subsequent sections of this addendum present the results of additional investigations with the Rulison flow and transport model. The overarching intention is to increase the usefulness of the model results for supporting decisions related to institutional controls and monitoring at the Rulison site by analyzing transport behavior in the upper tail of the distribution of original results.

Following this introduction, there are three main sections to the addendum. In the first, several key features of the original model are altered to examine their impact on tritium transport from the chimney to the production well. These include the partitioning of tritium between liquid and vapor phases, the porosity of hydraulic fractures surrounding the gas production well, the diffusivity for vapor movement in all rock types, and the water content of hydraulic fractures at the hypothetical production well. These investigations were conducted for a single realization (number 10) from Cooper *et al.* (2007), which was at the 99th percentile with respect to tritium mass reaching the production well. This means that only one percent of the simulations resulted in greater tritium mass reaching the well, in either the gas or liquid phases.

The second section presents additional analysis of the 10 simulations resulting in maximum transport from Cooper *et al.* (2007). These realizations (from the 500 generated in Cooper *et al.*, 2007) were rerun with the revised partitioning coefficient, hydraulic fracture porosity and diffusivity values. As there was interest only in simulations that exhibited tritium breakthrough to the well, and not on their statistics *per se*, there was little reason to re-run all 500 realizations because these realizations captured the greatest simulated transport.

Conclusions are presented in the final section to summarize the findings from the new model runs in the context of future site management.

As discussed below, many of the new realizations did not result in tritium breakthrough at the hypothetical production well. For discussion purposes, however, values of X_g^{THO} are reported in order to give the reader a feel for the relative values of the calculated tritiated water vapor mass fractions. Values of X_g^{THO} below the background value of 10^{-20} have no physical significance.

Examination of Key Model Features

Test simulations were run to investigate the significance of the tritium liquid-vapor partitioning coefficient, hydraulic fracture porosity, diffusivity, and hydraulic fracture water content on the spreading of tritium. These are discussed in separate sections below. These issues are examined for a single realization, number 10, of the 500 realizations reported by Cooper *et al.* (2007). Realization 10 was at the 99th percentile with respect to tritium mass fraction at the production interval, meaning that only one percent (five of the 500) of the simulations resulted in greater tritium mass fraction reaching the well, in either the liquid or gas phases. The location of the well in the simulations is 258 m west of the center of the nuclear chimney, as in Cooper *et al.* (2007). Figure 1a and b shows X_g^{THO} from the 2007 report for realization 10 for times 38 and 68 years after the detonation. This can be considered a “reference” simulation to compare changes in the key parameters. Additionally, mass fractions of tritium in the gas phase (tritiated water vapor) might more easily be thought of as the activity produced by a liter of condensed water vapor (pCi/L). A mass fraction of 1×10^{-20} is equivalent to the tritium background concentration of 4 pCi/L liquid equivalent (1 liter of water condensed from the gas phase would have an activity of 4 pCi/L), a mass fraction of 1×10^{-19} is equivalent to 40 pCi/L liquid equivalent, 1×10^{-18} is equivalent to 400 pCi/L liquid equivalent, and so forth.

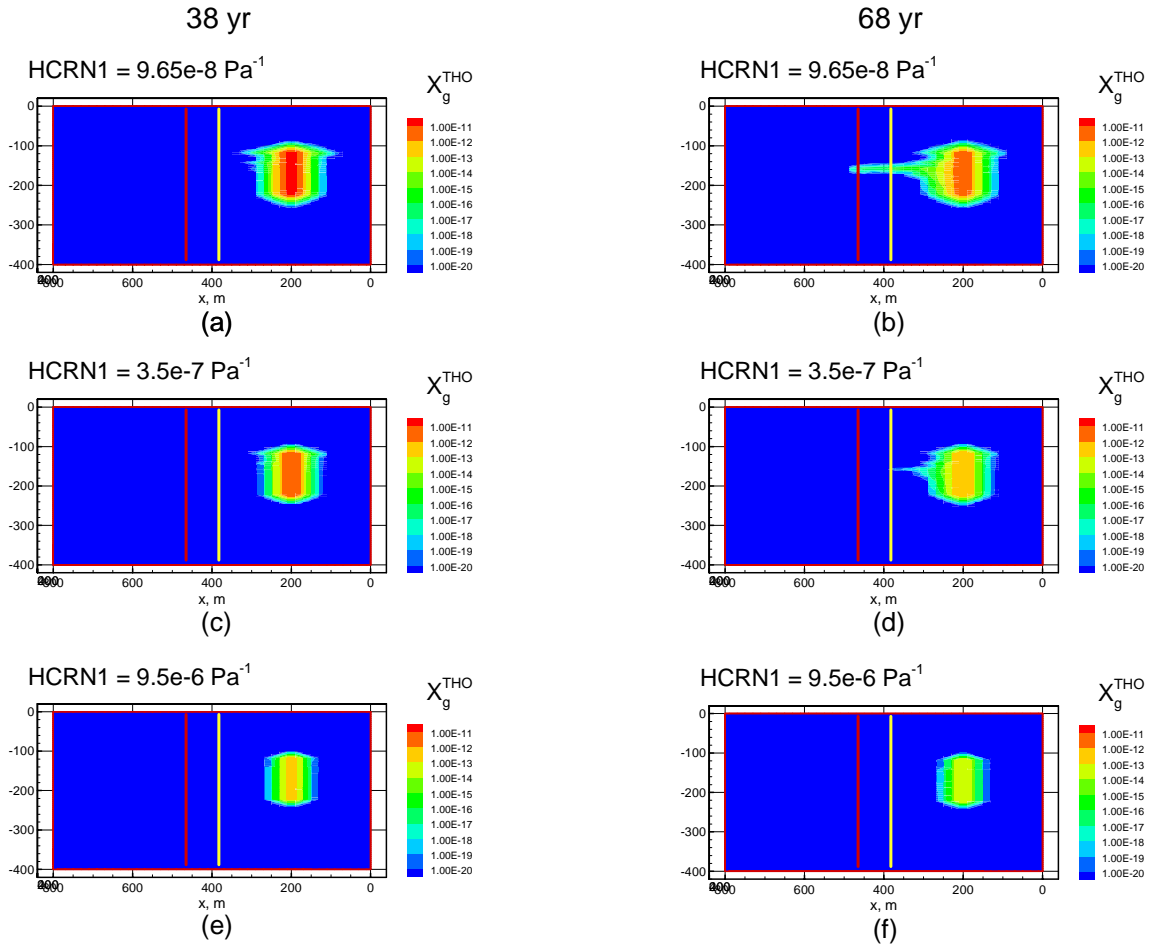


Figure 1. Results of three simulations in which the inverse Henry's law constant was changed. The three simulations used realization 10, which represents gas-phase tritium concentration at the 99th percentile in Cooper *et al.* (2007). The left-hand column shows the field of X_g^{THO} 38 years after the nuclear detonation while the right-hand column shows X_g^{THO} at 68 years. The first row, (a) and (b), shows the X_g^{THO} field for an inverse Henry's law constant appropriate for a temperature of 312°C, while the second row shows the results for exactly the same simulation but with the inverse Henry's law constant equivalent to a temperature of 230°C. The third row is the same as the first two, but for an inverse Henry's law constant appropriate for a reservoir temperature of 101°C. The yellow vertical line in each figure depicts the location of the lot 11/12 boundary while the red vertical line shows the location of the gas production well.

For the first 38 years of the simulation time, diffusion is the process responsible for tritium migration from the nuclear chimney. Figure 1a shows that diffusion is minimal and that prior to gas production, tritium is contained within lot 11 (the boundary between lots 11 and 12 is shown by the vertical yellow line). At 38 yr, gas production from the hypothetical well induces a pressure gradient toward the well; at this time transport is dominated by advective gas flow rather than diffusion. Gas production lasts for 30 yr when production is assumed to cease and the pressure field restores itself over the following several decades to the pre-production zero gradient (this is not shown in the figures but is discussed in the

original report). Figure 1b shows the tritium plume breaking through to the production zone in the well (the vertical red line in the figure) with $X_g^{THO} = 2.33 \times 10^{-19}$. Vertical diffusion is limited to within 40 m in the region between the farthest extent of the nuclear-generated fractures (extending 180 m from the center of the chimney) and the well. The path outlined by the presence of tritium (essentially a streamline running from the center of the chimney to the production well) is determined by the relationship between the connectivity of sand bodies and the location of the production interval in the well.

Tritiated Water Partitioning Coefficient

An important feature of the model is the partitioning of tritium (as THO) between the liquid and vapor phases of water. Liquid water is essentially immobile in the simulated subsurface conditions due to low relative permeability. In addition, the molecular diffusivity of tritiated water in the gas phase is about four orders of magnitude greater than in the liquid phase. These factors restrict significant migration of tritium to the gas phase. As tritiated water vapor moves through the subsurface pores, it continually partitions into liquid water across gas-water interfaces, which retards gas-phase tritium migration. As more tritium partitions into the liquid phase, less tritium is available for gas-phase migration.

The inverse Henry's law constant (H_c^{-1}) is the model parameter that controls the partitioning. A smaller value results in less partitioning and more tritium available for gas-phase migration, whereas a larger H_c^{-1} results in more tritium stored in the immobile liquid water. Cooper *et al.* (2007) used a trial-and-error approach to determine H_c^{-1} (the details are on pp. 51-54 of Cooper *et al.*, 2007). This procedure resulted in an H_c^{-1} value of $9.65 \times 10^{-8} \text{ Pa}^{-1}$. A literature review found one published value for the Henry's law constant (H_c) of 1.7×10^{-5} [dimensionless] at 20°C (Smiles *et al.*, 1995), which equates to an H_c^{-1} of $4.3 \times 10^{-4} \text{ Pa}^{-1}$, but it is unclear how to determine a value for reservoir temperatures. Given the importance of the partitioning and the higher subsurface temperature, the decision in Cooper *et al.* (2007) was to use the smaller derived H_c^{-1} value because it allowed greater tritium transport.

Recent work by Ron Falta (Clemson University, written communication) independently derives the inverse Henry's law constant for tritiated water and demonstrates that the Smiles *et al.* (1995) value is correct. Falta's derivation is provided in Appendix A. Note that the constant is related to the vapor pressure of water, which is dependent on temperature. As temperature increases, the inverse Henry's law constant decreases (Figure 2), favoring partitioning into the vapor phase. Temperature surveys performed in well R-EX prior to the nuclear test recorded a temperature of approximately 101°C (214°F) at a depth of 2560 m (8400 ft, Austral and CER, 1969). This coincides to an inverse Henry's law constant of $9.52 \times 10^{-6} \text{ Pa}^{-1}$ using Falta's derivation. Temperatures in the nuclear chimney estimated during production testing (less than a year after the detonation) were reported as high as 230°C (445°F) (Reynolds Jr., 1971). The estimated inverse Henry's law constant for that temperature is $3.5 \times 10^{-7} \text{ Pa}^{-1}$.

The inverse Henry's law constant used by Cooper *et al.* (2007) corresponds to the unreasonably high subsurface temperatures of over 300°C (almost 600°F), and results in a maximum X_g^{THO} value of 2.33×10^{-19} at the production well at 68 years. When the value corresponding to the in situ formation temperature of approximately 101°C is used, no tritium transport is observed to the production well (Figure 1 e and f). If the partitioning value corresponding to the peak chimney temperature is used, transport is observed, but not

to the degree shown in Cooper *et al.* (2007) (Figure 1c and d). The maximum X_g^{THO} value is less than background (3.3×10^{-21}) when using the H_c^{-1} value for 230°C.

The study of nuclear tests on the Nevada Test Site (NTS) has indicated that after cavity collapse, test heat is mostly concentrated in the melt glass, with some residual heat in portions of the former cavity subsequently filled with rubble (Carle *et al.*, 2003). The persistence of the residual heat depends largely on permeability, with one low-permeability example from the NTS expected to require hundreds of years for the melt glass zone to cool. Thus, the tritium partitioning in the upper portion of the Rulison chimney and throughout the surrounding formation is best represented by H_c^{-1} at 101°C, though partitioning in the lower portion of the Rulison cavity may be under conditions represented by H_c^{-1} at 230°C.

The subsequent sensitivity analyses were performed with H_c^{-1} values for both 101°C and 230°C. The influence of other parameters is most readily seen when some transport occurs, so the figures and discussion tend to focus on the results using H_c^{-1} for 230°C.

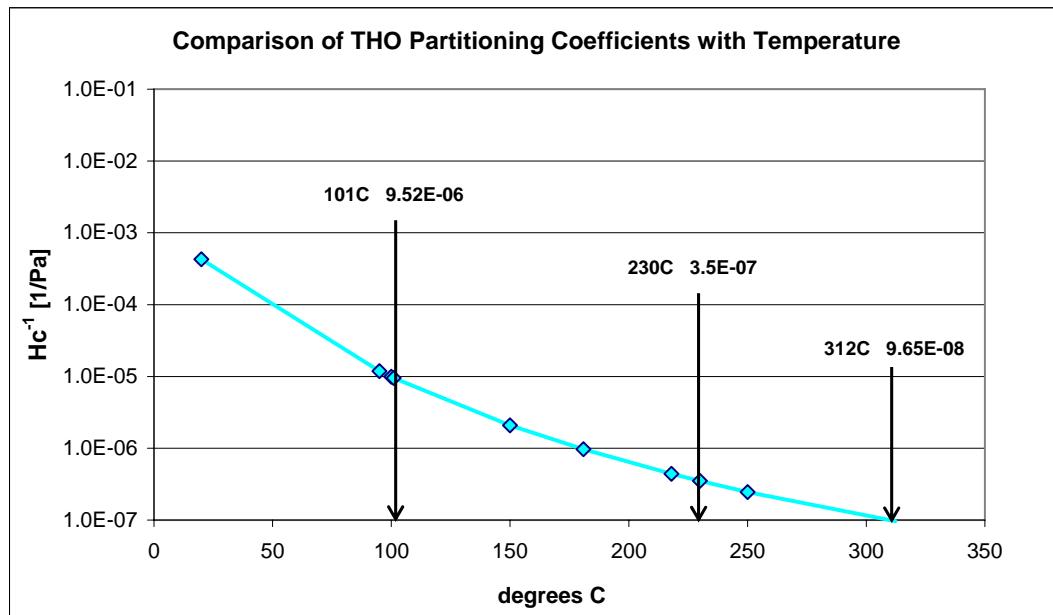


Figure 2. Temperature dependence of the inverse Henry's law constant (H_c^{-1}) for tritiated water partitioning between liquid and gas phases. Smaller H_c^{-1} values result in less partitioning into the liquid.

Hydrofracture Porosity

Porosity is a measure of the volume of void space in a rock relative to the volume occupied by solid material. Though higher porosity is often (but not always) associated with higher permeability, it also leads to lower fluid velocity. This can be readily visualized by considering two sizes of pipes; water must move faster through the smaller pipe in order to discharge the same gallons per minute as a larger pipe. As a result, smaller porosity values lead to faster contaminant velocity.

The original simulations assumed that the hydrofractures (hydraulically generated fractures surrounding the production well) could be represented by an equivalent porous medium with a porosity of 0.10. Based on data reported from production wells completed in

the Mesaverde Group in the Piceance Basin, and data from hundreds of cores from the Williams Fork Formation at the MWX site, a range of 0.0008 to 0.105 (normal distribution with a mean of 0.0529) was used in the Rulison model for porosity of the naturally fractured sandstone reservoir. The sandstone of the hydraulically fractured zone adjacent to the hypothetical production well is expected to have a higher porosity than the naturally fractured sandstone, particularly given the widespread use of proppants. Proppants are solid material, usually well-sorted sand, injected with the hydraulic fracturing fluid to hold the fracture open. The value of 0.10 used in the original simulations ensured that the hydrofractures would have a porosity at least as high as the adjacent sandstone. An alternative to this is to assume that the hydrofracturing procedure enhances permeability but not porosity. For a realization with a lower porosity value from the native sandstone range, this will result in faster advective velocity.

A case in which the porosity of the hydrofractures is assumed to be the same as the native value of the sandstone (0.01275 for this particular realization) is shown in Figure 3. The H_c^{-1} value appropriate for 230°C is used because essentially no transport occurs with the value at 101°C. Focused flow through the sandstone toward the well is observed for both the reference case (with the hydrofracture porosity of 0.10), and for the tested case with the hydrofracture porosity nearly 1 order of magnitude smaller. The mass fraction of tritiated water in the gas phase is higher in Figure 3d than in Figure 3b due to the smaller porosity of the hydrofractures and resulting faster flow. The maximum X_g^{THO} in Figure 3d is 1.75×10^{-18} .

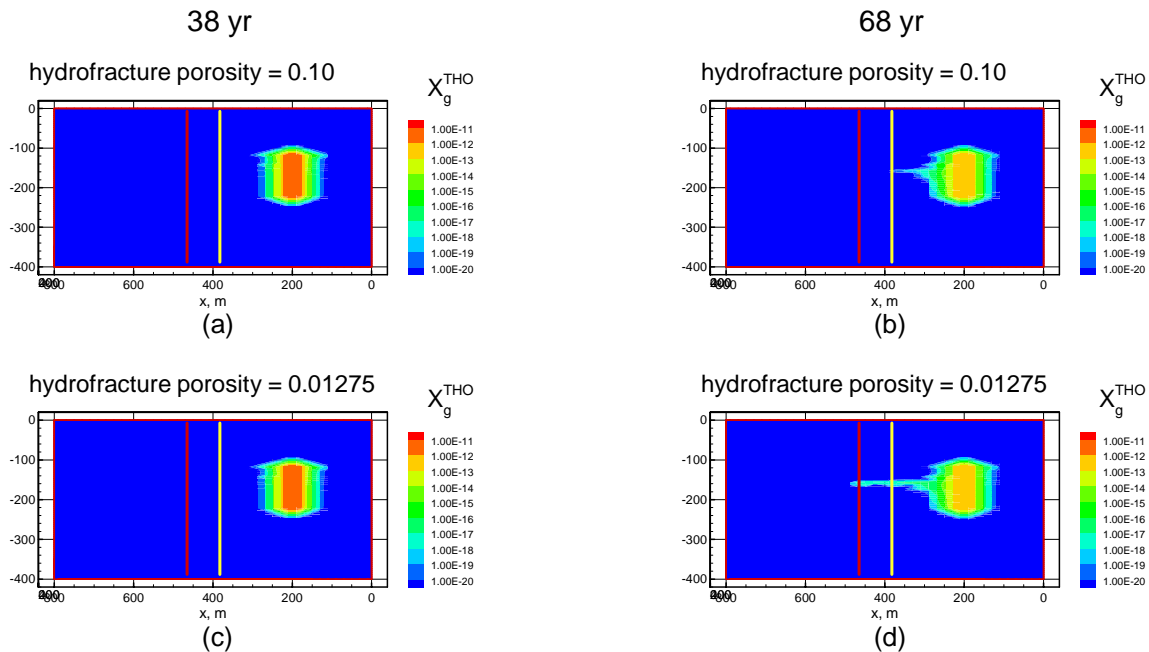


Figure 3. Results of two simulations that compare the effect of different hydrofracture porosity, based upon realization 10, and using partitioning for 230°C. The upper row shows gas-phase tritium mass fraction toward a production well in which the EPM hydrofracture porosity is 0.10, while the lower row shows the same mass fraction field with a hydrofracture porosity equivalent to that of the native sandstone, in this case 0.01275. The yellow vertical line in each figure depicts the location of the lot 11/12 boundary while the red vertical line shows the location of the gas production well.

Molecular Diffusivity and Tortuosity

Molecular diffusion of tritiated water vapor in the gas phase is the primary control on tritium migration from the Rulison cavity prior to, and after production from the gas well. Molecular diffusion is governed by Fick's first and second laws whereby diffusion is related to the concentration gradient and a diffusion coefficient, or diffusivity, for the chemical species. The rate of diffusion through the subsurface is less than in an open body of fluid because fluid, and the contaminants carried in fluids, can only move through the porous openings in the subsurface such that the route actually traveled has twists and turns around solid rock material. This effect is accounted for in computations by adjusting the diffusivity according to the porosity and tortuosity. Tortuosity represents the resistance to diffusion due to the influence of pore structure. It is the hydraulic parameter that accounts for the tortuous path, as compared to a nontortuous direct route. Tortuosity (τ) is essentially a multiplier on the diffusion coefficient with a range $0 < \tau < 1$. Smaller values indicate a more tortuous and longer route, while a value of 1 specifies no tortuosity such that diffusive transport is controlled entirely by the mass fraction gradient and diffusion coefficient for a particular phase.

In the original simulations, a Millington-Quirk model was used to determine the tortuosity effect on the diffusivity. It is the most commonly used model and is dependent upon porosity and phase saturation. The Millington-Quirk tortuosity is defined as $\tau = \phi^{1/3} S_\beta^{10/3}$, where ϕ is porosity and S_β is phase saturation. However, Millington-Quirk is strictly valid only for porous media, and therefore may suppress tritiated water vapor transport if flow is through less-tortuous fractures. A relative permeability-based model was investigated for the Rio Blanco nuclear test site (Cooper *et al.*, 2005) and resulted in slightly enhanced tritium transport, though not to a large degree.

In order to test a more conservative (than Millington-Quirk) constant-tortuosity value favoring gas-phase diffusion, a constant diffusivity approach to diffusion was adopted. This approach incorporates tortuosity as a multiplier to the gas and liquid phase diffusivities. The tortuosity value selected (0.047) is applied for all rock types and was determined from the Millington-Quirk equation, assuming the maximum value of porosity in the sandstone (0.105; Cooper *et al.*, 2007) and a value of 0.5 for aqueous phase saturation. This approach is conservative in that the larger porosity value equates to a less tortuous flow path.

A comparison of the two diffusion models for realization 10 (the same as Figure 1c and d) is shown in Figure 4, where Figures 4a and b show the Millington-Quirk-based model and Figures 4c and d show the constant diffusivity model. The higher tortuosity in the constant diffusivity case results in greater spread of tritium in all directions relative to the reference case. By 38 yr, tritium has diffused about 80 m farther than for the reference case. Breakthrough is observed at the well for both tortuosity models at 68 yr, with a wider breakthrough interval in the vertical direction for the constant-tortuosity model and greater mass fraction at the well. The X_g^{THO} at the production well at 68 yr in Figure 4d is 2.45×10^{-17} , in comparison to a peak value of 1.75×10^{-18} in Figure 4b. The growth of the diffusing parts of the plume (*e.g.*, in the vertical directions relatively unaffected by the production well) slows between 38 and 68 yr relative to earlier time, as transport is balanced by radioactive decay.

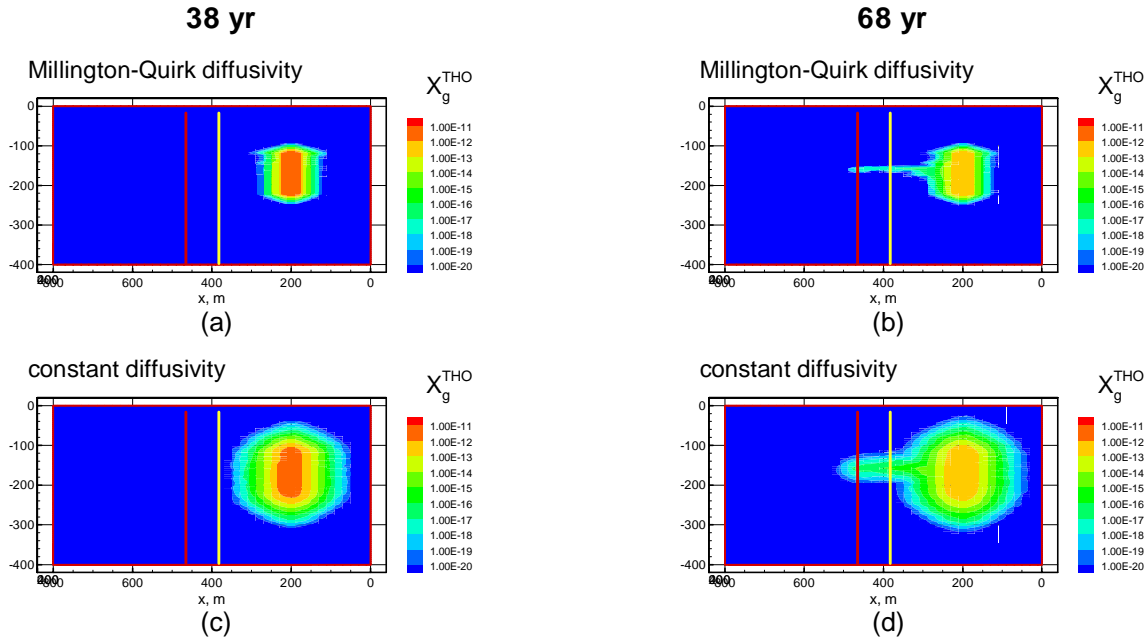


Figure 4. Results of two simulations in which the diffusivity model is compared. Realization 10 was used for both simulations. The left-hand column shows the field of X_g^{THO} 38 years after the nuclear detonation while the right-hand column shows X_g^{THO} at 68 years. The first row, (a) and (b), shows the X_g^{THO} field for a simulation in which the Millington-Quirk tortuosity model was used, while the second row shows the results for a similar simulation in which the diffusivity was assumed constant. The yellow vertical line in each figure depicts the location of the lot 11/12 boundary while the red vertical line shows the location of the gas production well.

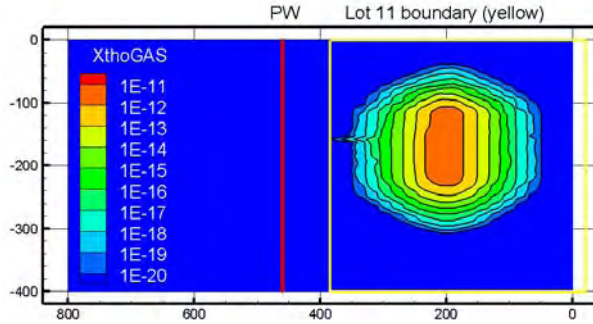
Liquid Water Content of Hydrofractures

Given the importance of tritium partitioning between the gas and liquid phases (described above), simulations were run to examine the effect of hydrofracture liquid saturation on transport. During gas production it is probable that the liquid content in the fractures extending from a production well is lower than that of the surrounding matrix, reducing the contact area between the phases and the subsequent partitioning of tritium from the mobile gas phase to the immobile liquid phase. In other words, dry hydrofractures may tend to increase tritium transport due to limited exchange between the mostly gas-filled fractures and the 50 percent liquid saturated matrix.

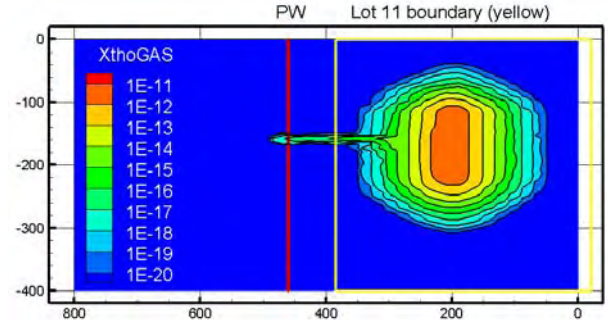
A comparison on the effects between “wet” and “dry” hydrofractures was made using realization 10, where the liquid saturation of the (EPM) hydrofracture grid blocks was set to 0.01 (as compared to the typical value of 0.50 used for all other simulations). During the 30-year gas production period, however, the hydrofracture grid blocks do not re-wet, due to the low relative permeability to liquid. The results, shown in Figure 5, indicate that hydrofracture liquid saturation is an important factor at early times but the effects become immaterial after several years of production. The tritium mass fraction migration results after 10 days of production (top row of Figure 5) are most dramatic for realization 10 because the hydrofractures are in direct contact with the nuclear fractures. The effect is reduced for realizations where the hydrofractures do not contact the nuclear fractures. Though apparently not important for overall tritium migration, this effect should be considered for sampling

procedures of wells drilled close to the detonation where hydrofractures and nuclear fractures could meet.

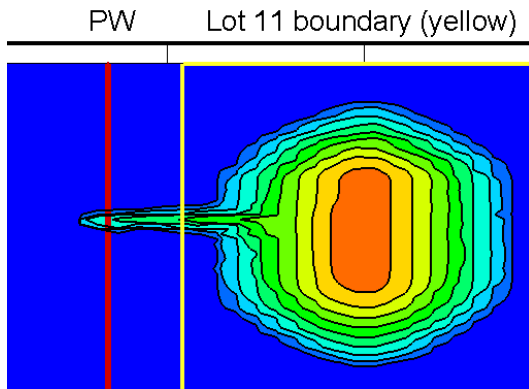
12 days (50% S_l)



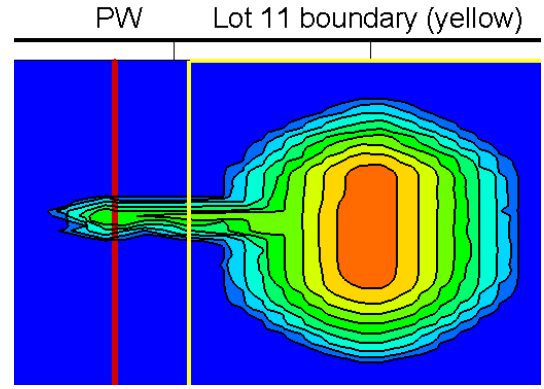
12 days (1% S_l)



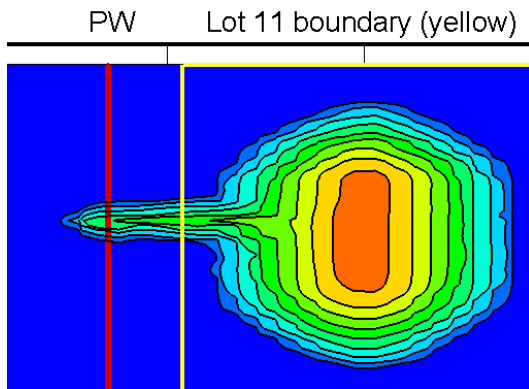
1 year (50% S_l)



1 year (1% S_l)



4 years (50% S_l)



4 years (1% S_l)

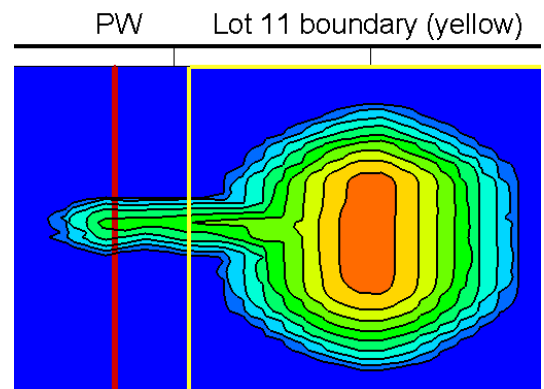


Figure 5. Results of two simulations that compare the effect of different hydrofracture liquid saturation (S_l), based upon realization 10. The left column shows gas-phase tritium mass fraction toward a production well in which the EPM hydrofracture liquid saturation is 0.50, while the right column shows the same mass fraction field with a hydrofracture liquid saturation of 0.01. The lower 2 rows are zoomed in for clarity.

Additional Model Simulations in Support of Site Institutional Controls

The analyses presented in the previous section indicate that the Rulison model of Cooper *et al.* (2007) can be improved by considering a Henry's law constant more appropriate for the subsurface temperature environment. In addition, the model was improved by changing the porosity of the hydrofractures to that of the naturally fractured sandstone where they occur and by enhancing diffusion through an updated tortuosity model.

The equally probable realizations of sandstone and shale geometry in the subsurface complicate simple extrapolation of the effects of changing model parameters. For this reason, the combined impact of changing the partitioning, hydrofracture porosity, and diffusivity was assessed for the ten realizations from Cooper *et al.* (2007) that allowed the most transport to the hypothetical production well located 258 m from the nuclear test. Parameters for these realizations are summarized in Table 1.

Table 1. Monte Carlo realization number (NMC), sandstone permeability (k_x and k_y) and porosity, and hydrofracture lengths and permeabilities for the 10 realizations resulting in the most breakthrough at the hypothetical production well.

NMC	k_x (m ²)	k_y (m ²)	Porosity	Anis. ratio	Hyfrc length (m)	k_{x_hyfrc} (m ²)	k_{y_hyfrc} (m ²)
10	3.65×10^{-17}	4.68×10^{-19}	0.0127	78	162	3.65×10^{-15}	4.68×10^{-17}
30	2.77×10^{-16}	2.92×10^{-18}	0.0269	95	81	2.77×10^{-14}	2.92×10^{-16}
80	2.04×10^{-16}	3.77×10^{-18}	0.0042	54	54	2.04×10^{-14}	3.77×10^{-16}
118	5.99×10^{-17}	7.07×10^{-19}	0.066	85	47	5.99×10^{-15}	7.07×10^{-17}
143	1.93×10^{-16}	1.95×10^{-18}	0.0155	99	52	1.93×10^{-14}	1.95×10^{-16}
185	7.80×10^{-17}	2.00×10^{-18}	0.0008	40	71	7.8×10^{-15}	2.0×10^{-16}
303	4.79×10^{-17}	1.48×10^{-18}	0.0031	32	68	4.79×10^{-15}	1.48×10^{-16}
321	1.88×10^{-16}	2.07×10^{-18}	0.0397	91	77	1.88×10^{-14}	2.07×10^{-16}
372	6.93×10^{-16}	7.36×10^{-18}	0.0066	94	90	6.93×10^{-14}	7.36×10^{-16}
493	6.42×10^{-17}	6.94×10^{-19}	0.0146	93	38	6.42×10^{-15}	6.94×10^{-17}

Table 2 shows that the peak tritium mass fractions in the gas phase (X_g^{THO}) at the production well for these realizations varied from 5.64×10^{-20} to 1.48×10^{-17} in the simulations reported in Cooper *et al.* (2007). When using the partitioning coefficient appropriate for the observed subsurface temperature, applying the native sandstone porosity for the hydraulic fractures, and using a constant diffusivity, all X_g^{THO} values are orders of magnitude below the background value of 10^{-20} . The constant diffusivity and hydraulic fracture porosity changes both serve to increase transport, but their effect is overwhelmed by the impact of the tritiated water partitioning coefficient. When the partitioning coefficient is adjusted to a value consistent with the nuclear cavity (which may not be representative of the upper chimney, nor the surrounding formation), the diffusivity and porosity effects are observed because the peak X_g^{THO} values are higher than those calculated in Cooper *et al.* (2007). This occurs for about half of the realizations, whereas for the other half, the Cooper *et al.* (2007) values are the highest of all the simulations. It appears that many of the realizations with very low sandstone porosities are more affected by changing the hydrofracture porosity to the native sandstone value, than are realizations with higher sandstone porosity.

Table 2. Peak tritium mass fraction in the gas phase (X_g^{THO}) at the production well location for the 10 Monte Carlo realizations with the most transport. Peak values occur between 48 and 68 years after the nuclear test. Three model results are shown for each realization: the results from Cooper *et al.* (2007); results with H_c^{-1} for 101°C, lower hydrofracture porosity, and constant diffusivity; and results for H_c^{-1} for 230°C, lower hydrofracture porosity, and constant diffusivity.

NMC	Cooper <i>et al.</i> (2007) _x (X_g^{THO})	$H_c^{-1}=101^\circ\text{C}$ _y (X_g^{THO})	$H_c^{-1}=230^\circ\text{C}$ (X_g^{THO})
10	2.33×10^{-19}	$\sim 10^{-30}$	9.25×10^{-17}
30	3.38×10^{-19}	$\sim 10^{-35}$	1.79×10^{-20}
80	5.48×10^{-18}	$\sim 10^{-30}$	5.10×10^{-17}
118	6.58×10^{-20}	$\sim 10^{-39}$	8.58×10^{-23}
143	1.08×10^{-19}	$\sim 10^{-37}$	1.53×10^{-19}
185	2.77×10^{-19}	$\sim 10^{-27}$	3.95×10^{-16}
303	5.64×10^{-20}	$\sim 10^{-30}$	6.83×10^{-17}
321	2.16×10^{-18}	$\sim 10^{-37}$	1.07×10^{-20}
372	1.48×10^{-17}	$\sim 10^{-30}$	6.99×10^{-18}
493	1.09×10^{-19}	$\sim 10^{-36}$	3.62×10^{-20}

Summary and Discussion

This addendum continues the Cooper *et al.* (2007) investigation into the transport of tritiated water vapor from the nuclear test at Project Rulison. Transport during a 38-year period following the detonation in 1969 until the year 2007 is examined, along with transport predictions for the cases of future natural gas production from a single hypothetical well located 258 m from the working point of the nuclear detonation.

The partitioning coefficient distributing tritiated water between the liquid and vapor phases is a critical component of the model. The value used in Cooper *et al.* (2007) is determined to be inappropriate for the simulations because it represents partitioning under much higher temperature conditions than encountered in the Rulison subsurface environment. Using a partitioning coefficient for the ambient subsurface temperature favors tritiated water in the immobile liquid phase to the extent that only limited migration is predicted away from the nuclear chimney. A coefficient appropriate for the temperature at the base of the nuclear chimney, where residual heat from the nuclear test may still persist, will overestimate vapor-phase tritium outside the chimney. Nonetheless, that partitioning coefficient also results in significantly less transport than estimated by Cooper *et al.* (2007).

Two other model aspects were modified in an effort to better represent the porosity of hydraulic fractures in the vicinity of the hypothetical production well as well as the diffusion of tritiated water. The values used for hydrofracture porosity and diffusivity have important consequences for the model outcome. Large values of tortuosity enhance diffusion while small values of porosity speed advection. Despite the rationale for the choice of parameter values in Cooper *et al.* (2007), different values of hydrofracture porosity and diffusivity were investigated to determine the effect on tritium migration. A hydrofracture porosity (in an EPM sense) less than that used in the Cooper *et al.* (2007) report increases gas-phase velocities in the vicinity of the well, and this translates directly into higher mass fractions at

the production well. A constant diffusivity model, rather than the Millington-Quirk tortuosity model, results in significantly greater diffusive transport of tritium away from the nuclear test. This enhanced transport may not always correspond to higher tritium mass fraction because diffusive spreading can dilute the mass fraction by mixing in a larger volume of the subsurface. Although both effective porosity and tortuosity are important to transport, neither are easy to measure for fractured systems, and thus they are highly uncertain parameters that need to be carefully considered in future calculations.

Additional simulations are presented to consider the combined effect of the partitioning coefficient, hydraulic fracture porosity, and diffusivity. These are conducted using the ten realizations with the most transport in the Cooper *et al.* (2007) model. These realizations sample a small subset of the 500 equally probable combinations of sandstone and shale layers, and flow and transport parameters examined in the original model, but nonetheless allow a broader evaluation than provided by sensitivity analysis for one realization. These results reveal the dominant importance of the tritiated water partitioning coefficient. In all cases, using the partitioning coefficient appropriate for the natural subsurface environment, transport does not occur to any significant distance past the nuclear fractured zone. When the partitioning coefficient is adjusted to higher temperature, as could be encountered very close to the nuclear melt glass, the combined impact of constant diffusivity and reduced hydrofracture porosity increase transport relative to the original model results. Even with the higher partitioning coefficient, several of these top ten realizations experience transport only slightly above background at the production location. Therefore, it is likely that none of the remaining 490 realizations (of the original 500) would have resulted in transport to the well.

These results, when viewed together with those presented in Cooper *et al.* (2007), enhance understanding of the degree to which the various hydraulic parameters affect transport of gaseous radionuclides at the Rulison site. The revised parameters are believed to be an improved representation of the Rulison subsurface, but their application does not substantively change the conclusions of Cooper *et al.* (2007) of a low probability of significant tritium transport to a production well located 258 m west of the nuclear test.

Because the new simulations focused on a subset of the original realizations, the importance of the sandstone-shale geometry is not apparent in the result. The ten realizations with the most transport were used, and all of these had well-connected sandstone between the nuclear chimney and the production well. Many more of the 500 realizations did not have continuous sandstone connections and allowed little to no transport toward the production well. Based on the results in Cooper *et al.* (2007), the primary controlling factor for whether or not tritium migrates to the well is the presence or absence of sandstone units connecting the nuclear chimney and the production well. If those connections exist for a given realization (a probability found to be small in Cooper *et al.* 2007), other parameters come into play. The work in this addendum indicates that the most important of these other model features is the partitioning of tritiated water between vapor and liquid phases. The porosity of hydraulic fractures and diffusivity are also important, but secondary to the partitioning.

Further investigation could increase confidence in the results by lowering uncertainty. Additional information regarding the sandstone and shale geometry is of primary importance for calculations regarding migration to future production wells, and can be gained by log analysis of nearby wells and more sophisticated representations of hydrofacies units (*e.g.*, subunits within stacked sandstone point bars). Fractures and critical related properties such as

porosity could be explicitly included in the model domain, and uncertainty in diffusivity included in the Monte Carlo uncertainty analysis. Fracture flow can be implemented in TOUGH2, although it introduces additional, unknown parameters in the simulations. Probability distributions, however, could be developed for these parameters (primarily capillary pressure and relative permeability curves in fractures) and could be included in additional Monte Carlo simulations, which would also include rock tortuosity as a random variable. Other enhancements that could be implemented to increase realism in the model are simulation of gas production using defined pressures rather than a defined production rate, and refinement of the permeability assignments to account for within-sand-body permeability variations.

References

- Austral Oil Company and CER Geonuclear, 1969. Project Rulison – Site Evaluation Pre-Shot R-EX Well Test Data. Project Report PNE-R-7.
- Carle, S.F., R.M. Maxwell, and G.A. Pawloski, 2003. Impact of Test Heat on Groundwater Flow at Pahute Mesa, Nevada Test Site. Lawrence Livermore National Laboratory report UCRL-ID-152599.
- Cooper, C.A., M. Ye, J. Chapman, and C. Shirley, 2005. Radionuclide Migration at the Rio Blanco Site, A Nuclear-Stimulated Low-permeability Natural Gas Reservoir. Desert Research Institute Report No. 45215.
- Cooper, C.A., Ye, M., and J. Chapman, 2007. Tritium Transport at the Rulison Site, a Nuclear-Stimulated Low-Permeability Natural Gas Reservoir, Desert Research Institute Report No. 45224, 102 pp. *Same as* U.S. Department of Energy (DOE) Office of Legacy Management, 2007. DOE/NV/13609-54, DOE M/1522 2007.
- DeGolyer and MacNaughton Co., 1971. Report on Interpretation of Test Data for Project Rulison in the Rulison Field, Garfield County, Colorado. Prepared for Austral Oil Co.
- Reynolds Jr., M., 1971. Project Rulison Summary of Results and Analyses. American Nuclear Society Winter Meeting, PNE-R-55.
- Smiles, D.E., Gardner, W.R., and R.K. Schulz, 1995. Diffusion of tritium in arid disposal sites, *Water Resour. Res.*, 31(6), 1483-1488.

Appendix A: Calculation of HCRN1 in EOS7R to represent tritiated water (THO) partitioning between the gas and aqueous phases

Ron Falta 4/23/08

Representing the tritium in EOS7R as component RN1, assume that the tritium is only present in the form of tritiated water vapor (THO). The THO behaves like water, and can evaporate into the gas phase. It is known that water vapor condensed from gas samples has the same mass fraction of tritiated water as the adjacent aqueous phase. We can reproduce this behavior in EOS7R using Henry's law by choosing the Henry's partition coefficient HCRN1 so that it gives these same mass fractions. By definition

$$HCRN1 = \frac{\chi_l^{THO}}{P_g^{THO}}$$

where χ_l^{THO} is the mole fraction of tritiated water in the aqueous phase, and P_g^{THO} is the partial pressure of tritiated water vapor in the gas phase.

In the gas phase, the ratio of tritiated water molecules to regular water molecules should be the same as in the aqueous phase; this implies that the ratio of the tritiated water vapor partial pressure to the regular water partial pressure should be the same as the aqueous mole fraction of tritiated water:

$$\frac{P_g^{THO}}{P_g^{H_2O}} = \chi_l^{THO}$$

At equilibrium, the water vapor partial pressure is equal to the water saturated vapor pressure, so the tritiated water vapor partial pressure should be

$$P_g^{THO} = \chi_l^{THO} P_{vap}^{H_2O}$$

Substituting, HCRN1 should be calculated as

$$HCRN1 = \frac{1}{P_{vap}^{H_2O}}$$

so HCRN1 is simply the inverse of the water vapor pressure at the prevailing temperature. At a temperature of 100°C, $HCRN1 = 1/101325 = 9.869 \times 10^{-6} \text{ Pa}^{-1}$.

This was tested in EOS7R by running a simple 1 gridblock problem. Using a volume of 1 m³ and a porosity of 0.35, the problem is initialized with a pressure of 200 bar, a temperature of 100°C, and an initial tritiated water aqueous mass fraction of 1x10⁻⁷. The TOUGH2 mass balance table shown below demonstrates that the aqueous mass fraction of tritiated water is 1x10⁻⁷, as expected (add the dissolved air to get the total aqueous mass).

```

THE TIME IS 0.000000E+00 SECONDS, OR 0.000000E+00 DAYS
      COMPONENT MASS IN PLACE (KG)
*****
      PHASES *      GAS      AQUEOUS      ADSORBED      TOTAL
*****
COMPONENTS *
WATER      * 0.20920541E-01 0.33751524E+02 0.00000000E+00 0.33772444E+02
BRINE      * 0.00000000E+00 0.00000000E+00 0.00000000E+00 0.00000000E+00
RN1        * 0.20622172E-08 0.33859701E-05 0.00000000E+00 0.33880323E-05
RN2        * 0.00000000E+00 0.00000000E+00 0.00000000E+00 0.00000000E+00
AIR        * 0.65008184E+01 0.10817398E+00 0.00000000E+00 0.66089924E+01
*****

```

In the gas phase, the mass of tritiated water vapor, 2.0622x10⁻⁹ kg divided by the regular water vapor mass of 2.09205x10⁻² gives a mass fraction of 0.986x10⁻⁷, which is very close to the aqueous mass fraction of 1x10⁻⁷. This ratio is correctly maintained throughout the simulation.

The equivalent dimensionless Henry's constant, $H = C_g^{THO} / C_l^{THO}$ can be derived in the same way. Since the ratio of tritiated water vapor to regular water vapor in the gas phase is the same as the mass fraction of tritiated water in the aqueous phase,

$$C_g^{THO} = X_l^{THO} C_g^{H_2O}$$

Since the mass concentration of tritiated water in the aqueous phase is the tritiated water mass fraction multiplied by the water density, Henry's constant can be written as

$$H = \frac{X_l^{THO} C_g^{H_2O}}{X_l^{THO} \rho_l} = \frac{P_{vap}^{H_2O} M_{wt}^{H_2O}}{zRT \rho_l}$$

using the vapor pressure of water, and the real gas law. Computing H for tritiated water at a temperature of 20°C gives a value of 17x10⁻⁶, which is the same as that reported by Smiles *et al.* (1995). Note that this approach is mathematically equivalent to the TOUGH2 EOS7R approach for partitioning the tritiated water.